Boundary-Layer Meteorol (2010) 134:257–267
DOI 10.1007/s10546-009-9450-y

ARTICLE

Bulk Transfer Relations for the Roughness Sublayer

Koen De Ridder

Received: 16 September 2008 / Accepted: 5 November 2009 / Published online: 1 December 2009
© Springer Science+Business Media B.V. 2009

Abstract In the roughness sublayer (RSL), Monin–Obukhov surface layer similarity theory fails. This is problematic for atmospheric modelling applications over domains that include rough terrain such as forests or cities, since in these situations numerical models often have the lowest model level located within the RSL. Based on empirical RSL profile functions for momentum and scalar quantities, and scaling the height with the RSL height z_*, we derive a simple bulk transfer relation that accounts for RSL effects. To verify the validity of our approach, these relations are employed together with wind speed and temperature profiles measured over boreal forest during the BOREAS experimental campaign to estimate momentum and heat fluxes. It is demonstrated that, when compared with observed flux values, the inclusion of RSL effects in the transfer relations yields a considerable improvement in the estimated fluxes.

Keywords Atmospheric numerical modelling · Roughness sublayer · Surface-layer transfer relations

List of symbols

C_D	Drag coefficient for momentum
C_H	Drag coefficient for heat
d	Displacement height (m)
h	Canopy height (m)
i	Index indicating momentum (M) or heat (H) transport
k	von Kàrmàn constant
L	Obukhov stability length (m)
L_s	Aerodynamic canopy length scale (m)
u	Wind speed (m s^{-1})

K. De Ridder (✉)
VITO—Flemish Institute for Technological Research, Boeretang 200, 2400 Mol, Belgium
e-mail: koen.deridder@vito.be

u_h	Wind speed at canopy top (m s^{-1})
u_*	Friction velocity (m s^{-1})
z	Height above the displacement height ($z = Z - d$) (m)
z_*	Roughness sublayer height above the displacement height (m)
z_0	Aerodynamic roughness length (m)
z_{0H}	Roughness length for heat (m)
Z	Height above the ground (m)
Z_*	Roughness sublayer height measured from the ground (m)
α_i	Coefficient used in the stability functions
δ	Average inter-element spacing (m)
ϕ	Roughness sublayer profile function
η	Coefficient used in roughness sublayer function
$\Phi_{M,H}$	Surface-layer stability function for momentum, heat
χ	Height scaled with the roughness sublayer height ($\chi = z/z_*$)
ζ	Height scaled with the Obukhov length ($\zeta = z/L$)
λ	Coefficient in the approximated roughness sublayer correction
$\mu_{M,H}$	Coefficient in the approximated roughness sublayer correction
ν	Coefficient in the approximated roughness sublayer correction
$\psi_{M,H}$	Integrated stability function for momentum, heat
θ	Potential temperature (K)
θ_*	Surface-layer temperature scale (K)

1 Introduction

The atmospheric layer immediately above the canopy (roughness elements) constitutes the roughness sublayer (RSL). In this layer, turbulence is strongly affected by individual roughness elements, thus introducing an additional length scale, and standard Monin–Obukhov theory is no longer valid (Simpson et al. 1998). As a result, vertical profiles of wind speed and scalar quantities such as temperature and humidity deviate from profiles predicted by Monin–Obukhov surface-layer similarity theory, as confirmed, e.g., by Högström et al. (1989) over a pine forest. As a result, use of the classical flux–gradient relationships leads to erroneous flux estimates when using measurements taken near the canopy top. For instance, Mölder et al. (1999) found that turbulent flux estimates based on the gradient approach compared well to results from an eddy-correlation approach only when RSL effects were accounted for. The effect of the RSL on turbulent fluxes is important for a host of applications involving rough surfaces, including pollen dispersion over forests (Kuparinen et al. 2007), the determination of CO_2 fluxes (Simpson et al. 1998) and dry deposition fluxes (Neirynck and Ceulemans 2008) over forests from observed vertical gradients, the dispersion of pollutants emitted in the urban canopy (Rotach 1999), and the estimation of wind yield potential over cities (Ricciardelli and Polimeno 2006).

In three-dimensional (3D) numerical models of the atmosphere, ignoring RSL dynamics is problematic as the lowest model level is more often than not located within the roughness sublayer. Indeed, many models exhibit a lower level at 10 m or so, while their domains include rough land use types such as forests and cities, hence accounting for the RSL is mandatory (Luhar et al. 2006). Nevertheless, few models account for the roughness sublayer. To our best knowledge, the only mesoscale meteorological modelling exercise in which the RSL was accounted for is that conducted by Physick and Garratt (1995). Their approach involved an integral of a more or less complicated function which, in the absence of a closed-form

solution, required numerical integration. In the present paper, we derive a fairly simple analytical expression for use in atmospheric models, which accounts for the effect of the roughness sublayer.

The paper is organised as follows: in Sect. 2 the RSL profile function is specified and, based on these, bulk transfer relations are derived. The effect of the RSL on drag coefficients used in atmospheric models is quantified. The bulk transfer relations are then used in Sect. 3 to calculate turbulent surface heat and momentum fluxes over a boreal forest in Canada and verified against experimental flux measurements. Section 4 presents the conclusions.

2 Bulk Transfer Relations

2.1 RSL Profile Functions

In the atmospheric surface layer, vertical gradients of wind vector components and scalar quantities are generally expressed as empirical functions of relevant scaling variables, including the friction velocity (u_*), the scale of temperature fluctuations (θ_*) and the Obukhov length scale, defined as $L = u_*^2\bar{\theta}/kg\theta_*$, where $\bar{\theta}$ is the ambient potential temperature, k is the von Kàrmàn constant, and g is the acceleration due to gravity. In the roughness sublayer an additional length scale becomes relevant, viz, the height to which individual surface roughness elements affect the atmosphere. This RSL height, denoted Z_*, is not a well-defined quantity. (Note that in the remainder of this paper, capital Z will refer to height as measured from the ground surface, whereas z will be employed to denote the height above the displacement height, i.e., $z = Z - d$). Generally, it may be scaled with the canopy height h, the roughness length z_0, the displacement height d, the average horizontal inter-element spacing δ, or a combination of these. Arya (2001) mentions $Z_*/h \approx 1.5$–2.5, while Kaimal and Finnigan (1994) cite a value of 3 for this quantity; in a review paper, Raupach et al. (1991) found values in the range 2–5. Garratt (1978, 1980) found $Z_* \approx 3\delta$, and Cellier and Brunet (1992) proposed $Z_* \approx 4\delta + d$. In the context of 3D atmospheric modelling, the δ-based approach is somewhat problematic as, in general, no information is available regarding this quantity for typical modelling domains. Alternatively, Verhoef et al. (1997) employed $Z_* \approx h + 15z_0$. For tall vegetation, Graefe (2004) proposed $Z_* \approx h + 2.32L_s$, with $L_s \equiv u_h/(\mathrm{d}u_h/\mathrm{d}z)$ the aerodynamic canopy length scale (Raupach et al. 1996), u_h being the wind speed at the canopy top. Recently, Kuparinen et al. (2007) employed $Z_* \approx h + d$. Finally, it should be noted that, under stable conditions, the RSL height decreases considerably compared to the neutral and unstable values (Garratt 1983).

Monin–Obukhov surface similarity theory, extended to account for RSL effects, expresses the variation of wind speed (u) and potential temperature (θ) with height (z) as follows (see, e.g., Garratt 1992):

$$\frac{kz}{u_*}\frac{\partial u}{\partial z} \cong \Phi_M\left(z/L\right)\varphi_M\left(z/z_*\right), \tag{1}$$

and

$$\frac{kz}{\theta_*}\frac{\partial \theta}{\partial z} \cong \Phi_H\left(z/L\right)\varphi_H\left(z/z_*\right), \tag{2}$$

where Φ_M and Φ_H are empirical stability functions for momentum and heat (and other scalar quantities), respectively. In (1), the function $\phi_i(z/z_*)$, where subscript i is either heat (H) or momentum (M), accounts for roughness sublayer effects. Based on observations, Garratt (1978) proposed

$$\varphi_i\,(z/z_*) \approx e^{-0.7(1-z/z_*)}, \tag{3}$$

common for both momentum and scalar transport, and constrained to not exceed unity. Recent experimental work (Mölder et al. 1999; Graefe 2004) found observations to agree better with the expressions proposed by Cellier and Brunet (1992),

$$\varphi_i\,(z/z_*) \approx (z/z_*)^{\eta_i}\ , \tag{4}$$

again constrained to not exceed unity, and with $\eta_H \approx 1$ and $0.4 < \eta_M < 0.6$. The drawback of the above expressions is that they exhibit a non-physical discontinuity at $z = z_*$. Recognising this, Harman and Finnigan (2007, 2008), based on earlier work by Raupach et al. (1996), recently developed a physically-based profile function, which does not suffer from the discontinuity present in the profile functions mentioned above.

Here, we will also employ a continuous function, as follows:

$$\varphi_i\,(z/z_*) \approx 1 - e^{-\mu_i z/z_*}. \tag{5}$$

In order to fix the values of the empirical coefficients μ_i, we fitted the profile function (5) to data presented in Mölder et al. (1999), as shown in Fig. 1, and found that the best agreement with the data was obtained for $\mu_M \approx 2.59$ and $\mu_H \approx 0.95$. In fact, the fit obtained using (5) and these numerical values for μ_i exhibited lower root-mean-square deviations from the wind speed and temperature data than those encountered using the Cellier and Brunet (1992) relations. We would like to stress that we are not claiming that our profile relation (5) is superior to those of Cellier and Brunet (1992). In fact, we essentially prefer (5) as it presents the advantage of being continuous, and because it allows us to express the profile functions for both momentum and heat with a single functional form. Moreover, it allows use of one single value for the RSL depth scale for both momentum and heat, as the observed higher RSL heights for temperature (as compared to that for momentum) are accounted for by the different values of the empirical constants μ_M and μ_H.

2.2 Deriving Bulk Transfer Relations

For use in numerical atmospheric models, (1) is integrated from z_0 (or z_{0H}) to z, the latter corresponding to the first model level (reference level) above the surface, and $z_0(z_{0H})$ the

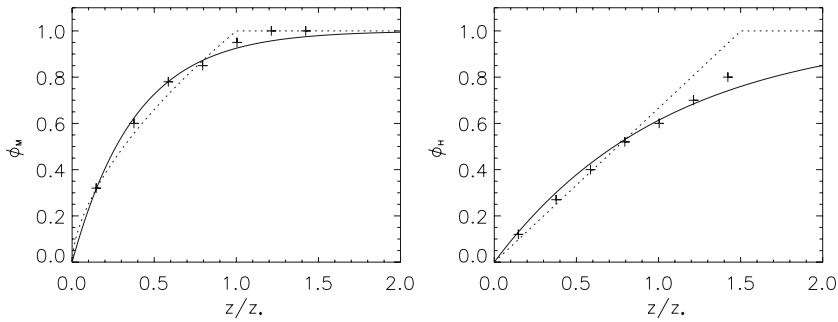

Fig. 1 RSL profile functions for momentum (*left*) and scalars (*right*) as a function of z/z_*. The *solid lines* represent (5) and the *dashed line* (3). The symbols ('+') correspond to experimental data presented in Mölder et al. (1999)

roughness length for momentum (heat). When including the roughness sublayer, this yields

$$u(z) = \frac{u_*}{k}\left[\ln(z/z_0) - \Psi_M(z/L) + \Psi_M(z_0/L) + \psi_M^*(z/L, z/z_*)\right], \tag{6}$$

and

$$\theta(z) - \theta_0 = \frac{\theta_*}{k}\left[\ln(z/z_{0H}) - \Psi_H(z/L) + \Psi_H(z_{0H}/L) + \psi_H^*(z/L, z/z_*)\right], \tag{7}$$

where θ_0 is the temperature at z_{0H}, Ψ_M and Ψ_H are the integrated stability functions, and with (Physick and Garratt 1995)

$$\psi_i^*(z/L, z/z_*) = \int_z^\infty \frac{\Phi_i(z'/L)}{z'}\left[1 - \varphi(z'/z_*)\right] dz'. \tag{8}$$

In the absence of a closed-form solution, Physick and Garratt (1995) approximated (8) using numerical integration. The remainder of this section focuses on finding a simple analytic expression for (8) such that numerical integration can be avoided. Adopting the functional form (5), (8) reduces to

$$\psi_i^*(z/L, z/z_*) = \int_z^\infty \frac{\Phi_i(z'/L)}{z'} e^{-\mu z'/z_*} dz'. \tag{9}$$

We derive an approximate expression to this integral by invoking the first mean value theorem for integration, which, in this particular case, asserts that there exists a value $\bar{z} \in [z, \infty[$ such that

$$\psi_i^*(z/L, z/z_*) = \Phi_i(\bar{z}/L) \int_z^\infty \frac{1}{z'} e^{-\mu z'/z_*} dz'. \tag{10}$$

The approximation made here is that we assume that $\bar{z} = z + \nu(z_*/\mu)$, with $\nu \in [0, \infty[$, which satisfies the requirement on the allowed domain for $\bar{z}$. The rationale behind this particular choice for $\bar{z}$ is that the latter's value is expected to lie somewhere between z (the lower bound of the integral) and $z + (z_*/\mu)$, which is the value at which the exponential function in the integrand becomes exponentially smaller than its value at the lower bound. The validity of this approximation, as well as the value for ν, will be determined later.

Equation (10) can now be written as

$$\psi_i^*(z/L, z/z_*) = \Phi_i\left[\left(1 + \frac{\nu}{\mu z/z_*}\right)\frac{z}{L}\right] E_1(\mu z/z_*), \tag{11}$$

in which E_1 is the exponential integral. The latter's so-called bracketing property (see (5.1.20) in Abramowitz and Stegun 1972) suggests that

$$E_1(x) \approx \frac{1}{\lambda}\ln\left(1 + \frac{\lambda}{x}\right) e^{-x}, \tag{12}$$

with $\lambda \approx 1.5$, thus finally yielding

$$\psi_i^*(z/L, z/z_*) \approx \Phi_i\left[\left(1 + \frac{\nu}{\mu z/z_*}\right)\frac{z}{L}\right]\frac{1}{\lambda}\ln\left(1 + \frac{\lambda}{\mu z/z_*}\right) e^{-\mu z/z_*}. \tag{13}$$

In this expression, ν is still an undetermined parameter. It was estimated by minimising, with respect to ν, the relative error on the calculated wind and temperature, expressed as

$$\frac{\Delta u}{u(z)} \equiv \frac{u(z) - \hat{u}\,(z, \nu)}{u(z)}, \tag{14}$$

and

$$\frac{\Delta \theta}{\theta(z) - \theta_0} \equiv \frac{\theta(z) - \hat{\theta}\,(z, \nu)}{\theta(z)}. \tag{15}$$

In the above expression, $u(z)$ and $\theta(z)$were calculated in an 'exact' manner using (6)–(8), together with numerical (Romberg) integration (Press et al. 1992) to evaluate ψ_i^*. The quantities $\hat{u}\,(z, \nu)$ and $\hat{\theta}\,(z, \nu)$ were calculated in a similar fashion, though using the approximate expression (13) for ψ_i^*. In these calculations we used the stability functions from Dyer (1974), given by

$$\Phi_H\,(z/L) = \Phi_M^2\,(z/L) = (1 - 16z/L)^{-1/2} \tag{16}$$

for $z/L < 0$, and

$$\Phi_H\,(z/L) = \Phi_M\,(z/L) = 1 + 5z/L \tag{17}$$

for $z/L > 0$, together with the corresponding Paulson (1970) integrated stability functions

$$\Psi_M\left(\frac{z}{L}\right) = \ln\left[\left(\frac{1+x^2}{2}\right)\left(\frac{1+x}{2}\right)^2\right] - 2\arctan x + \frac{\pi}{2}, \tag{18}$$

and

$$\Psi_H\left(\frac{z}{L}\right) = 2\ln\left(\frac{1+x^2}{2}\right), \tag{19}$$

with $x \equiv (1 - 16z/L)^{1/4}$, for $z/L < 0$. For stable conditions ($z/L > 0$), we have

$$\Psi_{H,M}(z/L) = -5z/L. \tag{20}$$

It was found that, in the range $0.2 < z/z_* < 3$ and $-5 < z/L < 1$, attributing values of $\nu \approx 0.5$ yielded the smallest relative differences on wind and temperature as expressed in (14), these differences never exceeding 4%. This is to be compared to the much larger error that is made when ignoring the RSL alltogether (i.e., ignoring the last term in (6) and (7)), in which case errors of up to 56 and 74% are found for momentum and heat, respectively.

2.3 Impact on Drag Coefficients

The modified bulk transfer relations, i.e., the relations (6)–(7) that take into account RSL effects on turbulent transport, have an effect on the drag coefficients used in atmospheric models. The drag coefficients for momentum and heat, defined as (Garratt 1992) $C_D \equiv [u_*/u(z)]^2$ and $C_H \equiv u_*\theta_*/\{u(z)[\theta(z) - \theta_0]\}$, respectively, were calculated using (6)–(7), once with and once without representing RSL effects.

The drag coefficients, plotted as a function of stability (as expressed by $z\,/\,L$), are shown in Fig. 2, for different values of z/z_*. As expected, the impact of including RSL effects is greater for low z/z_*. It can also be seen in Fig. 2 that the error made by approximating the integral constituting ψ_i^*, i.e., by using (13) to represent (10), is much smaller than the error

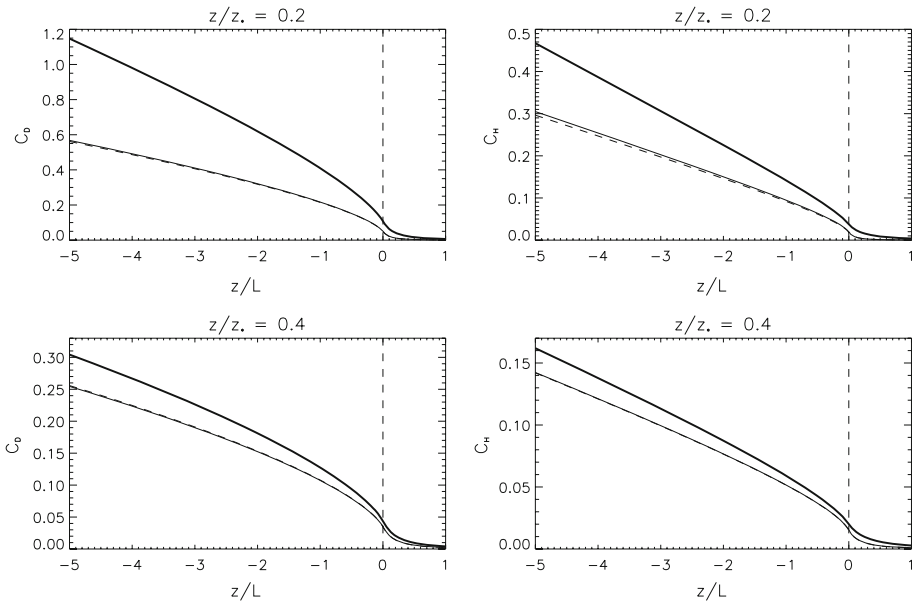

Fig. 2 Drag coefficients as a function of stability, without (*thick solid line*) and with (*thin solid line*) RSL effects taken into account, for momentum (*left*) and heat (*right*), for $z/z_* = 0.2$ (*upper panels*) and $z/z_* = 0.4$ (*lower panels*). The *dashed line* represents the drag coefficient accounting for RSL effects, but calculated in an 'exact' manner, i.e., using numerical integration instead of the approximation provided in (13)

made when ignoring RSL effects. Finally, it should be noted that the values used in Fig. 2 for z/z_*, i.e., 0.2 and 0.4, are quite representative of heights used for the lowest level in numerical atmospheric models applied over rough terrain. For instance, considering a forest with a mean tree height of 20 m, z_* would typically be of the order of 25 m, hence the ratios mentioned above for z/z_* correspond to model levels of 5 and 10 m.

3 Experimental Verification

As the RSL parameterisation developed above is subject to a certain degree of uncertainty, we verified its validity by comparing predicted turbulent surface momentum and sensible heat fluxes measured over a boreal forest during the Boreal Ecosystem-Atmosphere Study (BOREAS).

This experimental campaign took place in 1994 and 1996 in the northern boreal forests of Canada (Sellers et al. 1997). We employed data from the 30-m high flux tower (TF-08) located at the Old Jack Pine site (55.928°N, 98.588°W) in the Northern Study Area (NSA-OJP), as it provides measured temperature and wind speed profiles together with eddy-correlation estimates of the turbulent heat and momentum fluxes. We selected the period 29 July 1996 0500 UT to 5 August 1996 at 0500 UT, as it was characterized by good data coverage. All data used in this study were retrieved from the BOREAS data server (ftp://ftp.daac.ornl.gov/data/boreas/).

As the pine trees surrounding the flux tower are reported to be up to 13–14 m high (Bartlett et al. 2002), a value of $h = 13.5$ m was assigned to the vegetation height. Following Bartlett et al. (2002) we adopted a value of $d = 9$ m for the displacement height. An important issue is to fix the value of Z_* for the pine forest site. Mölder et al. (1999) found $Z_*/h \approx 2$

from their experimental data taken obtained over a pine forest. This figure is consistent with the formulation of Verhoef et al. (1997) that was mentioned in Sect. 2, yielding $Z_*/h \approx 2.1$ when using a representative value of $z_0/h \approx 0.071$ (Mölder and Lindroth 1999). It is also consistent with the Graefe (2004) expression (also see Sect. 2): since L_s/h values are typically in the range 0.3–0.6, a corresponding range of Z_*/h values is 1.7–2.4. Given all the above estimates, we adopt $Z_*/h \approx 2$ (hence $z_*/h \approx 2 - d/h$), which is also the mean of values cited by Arya (2001). The decrease of RSL height under stable stratification is accounted for using the parameterisation proposed by Physick and Garratt (1995).

We calculated friction velocity and sensible heat flux using the gradient method with wind speed measured by propeller-vane anemometers at 14.65 and 18.88 m above the forest floor, and temperature measured by transducer probes at 15.65 and 22.68 m. We further denote these measurement heights as $(z_1, z_2, z_3, z_4) \equiv (14.65, 15.65, 18.88, \text{and } 22.68\,\text{m})$.

The gradient calculation was carried out as follows: first we calculated a bulk Richardson number as

$$Ri_B = \frac{g z_1}{\theta_0} \frac{\theta(z_4) - \theta(z_2)}{[u(z_3) - u(z_1)]^2} \tag{21}$$

where one should note the 'staggered' character of Ri_B, caused by the different measurement heights used for temperature and wind speed. By using (6), and noting that $\zeta_i (\equiv z_i/L$, with $i \in \{2, 3, 4\})$ can be expressed as $\zeta_i = (z_i/z_1).\zeta_1$, one obtains a transcendental equation in the sole variable ζ_1, of the form $\zeta_1 = Ri_B f(\zeta_1)$. This equation was solved iteratively, using direct substitution (see, e.g., Koçak 2008), following the algorithm $\zeta_{1,n+1} = Ri_B f(\zeta_{1,n})$, with n the iteration step. By using again (6), together with the solution for ζ_1, u_* and θ_* were calculated, and also the sensible heat flux $H = -\rho c_p u_* \theta_*$, with ρ the air density (as calculated from measured air temperature and pressure using the ideal gas law), and $c_p = 1,004\ \text{J kg}^{-1}\ \text{K}^{-1}$ the heat capacity of the air at constant pressure. Friction velocity and turbulent sensible heat fluxes calculated as described above were compared to measured values, obtained by sonic anemometer at 30 m above the forest floor. Figure 3 shows the calculated versus the observed values.

From this figure, the beneficial effect of including RSL effects in the calculation is fairly clear, especially for the turbulent sensible heat flux, and to a lesser extent also for the friction velocity. This is confirmed quantitatively by the error statistics presented in Table 1. The mean absolute error (MAE) in the calculated sensible heat flux decreases from 78 to 29 W m^{-2} when accounting for RSL effects, and the bias reduces from −66 to −6 W m^{-2}. Accounting for RSL effects reduces the MAE of the calculated friction velocity from 0.17 to 0.13 m s^{-1}, and the bias reduces from −0.23 to −0.14 m s^{-1}.

4 Conclusions

We derived a simple expression to account for the influence of the roughness sublayer on flux-profile relationships, intended mainly for use in bulk surface transfer schemes in numerical atmospheric models. For completeness, the expression is reproduced here in compact form as

$$\psi_i^*(\zeta, \chi) = \Phi_i \left[\left(1 + \frac{\nu}{\mu_i \chi} \right) \zeta \right] \frac{1}{\lambda} \ln \left(1 + \frac{\lambda}{\mu_i \chi} \right) e^{-\mu_i \chi}, \tag{22}$$

with $\chi \equiv z/z_*$, $\zeta \equiv z/L$, $\mu_M \approx 2.59$, $\mu_H \approx 0.95$, $\nu \approx 0.5$, and $\lambda \approx 1.5$. This expression is fairly straightforward to implement in numerical codes. Indeed, significant portions of (22)

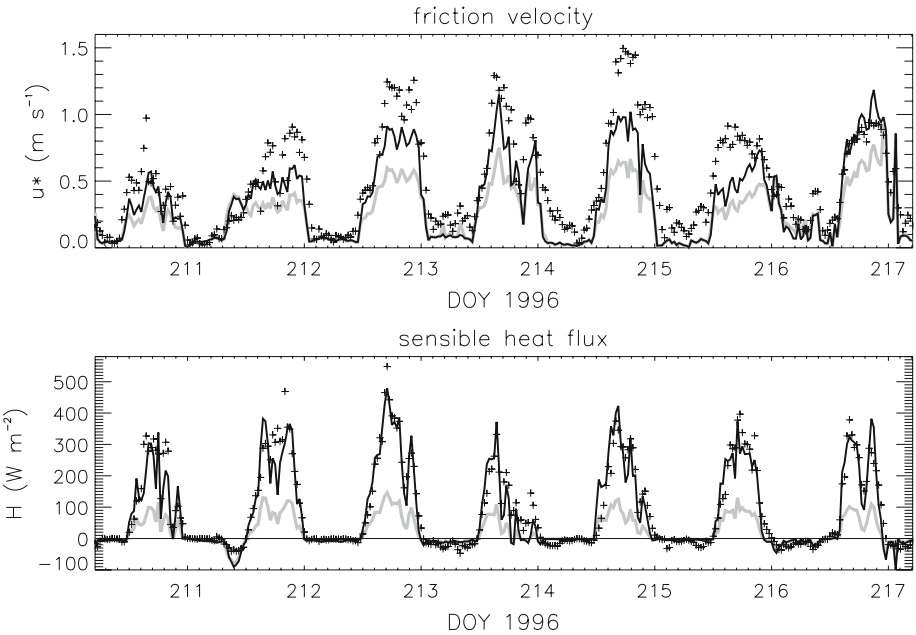

Fig. 3 Calculated (*solid lines*) versus observed (*symbols*) friction velocity (*upper panel*) and turbulent sensible heat flux (*lower panel*) for the BOREAS NSA–OJP site, for DOY 210-217 in 1996. The *black solid line* corresponds to the calculation accounting for RSL effects, the results shown as a *grey solid line* ignoring them

Table 1 Mean absolute error (MAE) and bias of calculated versus observed friction velocity and turbulent sensible heat flux, with versus without accounting for RSL effects

		u_*(m s^{-1})	H(W m^{-2})
MAE	With RSL	0.13	29
	Without RSL	0.17	78
BIAS	With RSL	−0.14	−6
	Without RSL	−0.23	−66

solely depend on the quantity $\mu_i \chi$, which in principle does not vary during a simulation, hence can be computed once for each surface grid cell, at the start of a model run. Furthermore, above a threshold of $z/z_* \gg 1$, i.e., essentially above surfaces with z_0 smaller than, say, 0.1 m, it is fair to simply set $\psi_i^* = 0$, since the exponential factor ensures this function vanishes very effectively with height.

The above expression was validated by comparing surface heat and momentum fluxes, calculated using the approach described above together with temperature and wind speed profiles measured over boreal forest during the BOREAS experimental campaign, with values measured by eddy correlation. It was demonstrated that, when compared to results obtained by ignoring RSL effects, our approach yielded a considerable improvement in the estimated fluxes.

Acknowledgements This research was conducted in the framework of the MUSTI project ("Measuring urban surfaces' thermal inertia"), with support from ESA's PRODEX programme and the Belgian Science

Policy Office. Part of the research was also conducted in the framework of the CLIMAQs project, with financial support of the Institute for the Promotion of Innovation by Science and Technology in Flanders (IWT-Flanders).

References

Abramowitz M, Stegun IA (1972) Handbook of mathematical functions with formulas, graphs, and mathematical tables, 10th printing. National Bureau of Standards, Washington, 1046 pp

Arya SP (2001) Introduction to micrometeorology, 2nd edition. Academic Press, San Diego, 420 pp

Bartlett PA, McCaughey JH, Lafleur PM, Verseghy DL (2002) A comparison of the mosaic and aggregated canopy frameworks for representing surface heterogeneity in the Canadian boreal forest using CLASS: a soil perspective. J Hydrol 266:15–39

Cellier P, Brunet Y (1992) Flux–gradient relationships above tall plant canopies. Agric For Meteorol 58: 93–117

Dyer AJ (1974) A review of flux-profile relationships. Boundary-Layer Meteorol 7:363–372

Garratt JR (1978) Flux profile relations above tall vegetation. Q J Roy Meteorol Soc 104:199–211

Garratt JR (1980) Surface influence upon vertical profiles in the atmospheric near-surface layer. Q J Roy Meteorol Soc 106:803–819

Garratt JR (1983) Surface influence upon vertical profiles in the nocturnal boundary layer. Boundary-Layer Meteorol 26:69–80

Garratt JR (1992) The atmospheric boundary layer. Cambridge University Press, UK, 316 pp

Graefe J (2004) Roughness layer corrections with emphasis on SVAT model applications. Agric For Meteorol 124:237–251

Harman IN, Finnigan JJ (2007) A simple unified theory for flow in the canopy and roughness sublayer. Boundary-Layer Meteorol 123:339–363

Harman IN, Finnigan JJ (2008) Scalar concentration profiles in the canopy and roughness sublayer. Boundary-Layer Meteorol 129:323–351

Högström U, Bergström H, Smedman A-S, Halldin S, Lindroth A (1989) Turbulent exchange above a pine forest, I: fluxes and gradients. Boundary-Layer Meteorol 49:197–217

Kaimal JC, Finnigan JJ (1994) Atmospheric boundary layer flows. Oxford University Press, Oxford, 289 pp

Koçak MC (2008) Simple geometry facilitates iterative solution of a nonlinear equation via a special transformation to accelerate convergence to third order. J Comput Appl Math 218:350–363

Kuparinen A, Markkanenb T, Riikonenb H, Vesalab T (2007) Modeling air-mediated dispersal of spores, pollen and seeds in forested areas. Ecol Model 208:177–188

Luhar A, Venkatram A, Lee S-M (2006) On relationships between urban and rural near-surface meteorology for diffusion applications. Atmos Environ 40:6541–6553

Mölder M, Lindroth A (1999) Thermal roughness length of a boreal forest. Agric For Meteorol 98–99:659–670

Mölder M, Grelle A, Lindroth A, Halldin S (1999) Flux-profile relationships over a boreal forest—roughness sublayer corrections. Agric For Meteorol 98–99:645–658

Neirynck J, Ceulemans R (2008) Bidirectional ammonia exchange above a mixed coniferous forest. Environ Pollut 154:424–438

Paulson CA (1970) The mathematical representation of wind speed and temperature profiles in the unstable atmospheric surface layer. J Appl Meteorol 9:857–861

Physick WL, Garratt JR (1995) Incorporation of a high-roughness lower boundary into a mesoscale model for studies of dry deposition over complex terrain. Boundary-Layer Meteorol 74:55–71

Press WH, Teukolsky SA, Vetterling WT, Flannery BP (1992) Numerical recipes in FORTRAN: the art of scientific computing, 2nd edition. Cambridge University Press, UK, 934 pp

Raupach MR, Antonia RA, Rajagopalan S (1991) Rough-wall turbulent boundary layers. Appl Mech Rev 44:1–25

Raupach MR, Finnigan JJ, Brunet Y (1996) Coherent eddies and turbulence in vegetation canopies: the mixing layer analogy. Boundary-Layer Meteorol 78:351–382

Ricciardelli F, Polimeno S (2006) Some characteristics of the wind flow in the lower urban boundary layer. J Wind Eng Ind Aerodyn 94:815–832

Rotach MW (1999) On the influence of the urban roughness sublayer on turbulence and dispersion. Atmos Environ 24–25:4001–4008

Sellers PJ, Hall FG, Kelly RD, Black A, Baldocchi D, Berry J, Ryan M, Ranson KJ, Crill PM, Lettenmaier DP, Margolis H, Cihlar J, Newcomer J, Fitzjarrald D, Jarvis PG, Gower ST, Halliwell D, Williams D, Goodison B, Wickland DE, Guertin FE (1997) BOREAS in 1997: experiment overview, scientific results, and future directions. J Geophys Res 102:28731–28769

Simpson IJ, Thurtell GW, Neumann HH, Den Hartog G, Edwards GC (1998) The validity of similarity theory in the roughness sublayer above forests. Boundary-Layer Meteorol 87:69–99

Verhoef A, McNaughton KG, Jacobs AFG (1997) A parameterization of momentum roughness length and displacement height for a wide range of canopy densities. Hydrol Earth Syst Sci 1:81–91